CRYSTAL GROWTH & DESIGN

Article

pubs.acs.org/crystal

Spatially Precise, Soft Microseeding of Single Protein Crystals by Femtosecond Laser Ablation

Hiroshi Y. Yoshikawa,*[,†,‡] Yoichiroh Hosokawa,*[,§] Ryota Murai,[‡] Gen Sazaki,[‡,∥] Tomoya Kitatani,[‡] Hiroaki Adachi,[‡,⊥] Tsuyoshi Inoue,[‡,⊥] Hiroyoshi Matsumura,[‡,⊥] Kazufumi Takano,[‡,⊥] Satoshi Murakami,[⊥,#] Seiichiro Nakabayashi,[†] Yusuke Mori,[‡,⊥] and Hiroshi Masuhara*[,§,▽]

[†]Department of Chemistry, Saitama University, Shimo-okubo 255, Sakura, Saitama 338-8570, Japan

[‡]Graduate School of Engineering, Osaka University, Yamadaoka 2-1, Suita, Osaka 565-0871, Japan

[§]Graduate School of Materials Science, Nara Institute of Science and Technology, Takayama 8916-5, Ikoma 630-0192, Japan

[∥]The Institute of Low Temperature Science, Hokkaido University, Sapporo 060-0819, Japan

[⊥]SOSHO Inc., Honmachi 1-6-18, Chuo-ku, Osaka 541-0053, Japan

[#]Graduate School of Bioscience and Biotechnology, Tokyo Institute of Technology, Nagatsuka 4259, Midori-ku, Yokohama, Kanagawa 226-8501, Japan

[▽]Department of Applied Chemistry and Institute of Molecular Science, National Chiao Tung University, Hsinchu 30010, Taiwan

ABSTRACT: We developed a spatially precise, soft microseeding method for the production of single protein crystals that are suitable for X-ray crystallographic studies. We used focused femtosecond laser pulses to produce, via multiphoton absorption processes, seed crystals from small regions (~1 μm^2) of crystals. Hen egg-white lysozyme seed crystals, produced in this manner, grew to be single crystals without any deterioration in their crystallinity. We also validated the technique using polycrystals for the membrane protein, acriflavine resistance protein B, for which single crystals are very difficult to obtain. In addition, we found that the shape of a tetragonal lysozyme crystal prepared from the seed could be controlled by altering the time interval between the initiation of crystallization and laser ablation. We also tried to comprehend the mechanism of femtosecond laser-induced microseeding. We visualized the ablated surfaces of the lysozyme crystals by atomic force microscopy and by laser confocal microscopy combined with differential interference microscopy. The results obtained in this study clearly demonstrate that femtosecond laser ablation of protein crystals is based on a photomechanical process, which ejects crystal fragments with little thermal damage. Femtosecond laser ablation is indeed very promising to produce high quality protein seed crystals from polycrystals or cracked crystals that are not suitable for X-ray diffraction studies.

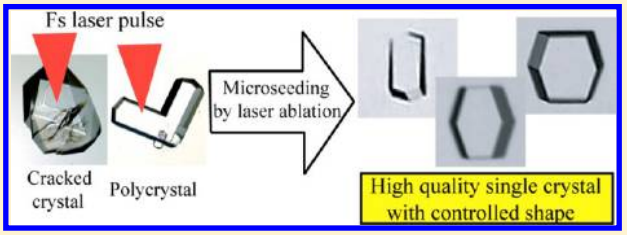

INTRODUCTION

High quality, single protein crystals that have a desirable shape are necessary for X-ray crystallographic structural studies. To obtain such protein crystals, many researchers have tried to adjust the environmental chemical and physical parameters, e.g., temperature, solvent, and cosolutes. However, irregularly shaped crystals, e.g., polycrystals and cracked crystals, that are not suitable for crystallography are often obtained. The only known method that can use the irregularly shaped crystals to produce crystals suitable for X-ray diffraction is microseeding, which usually involves manually crushing crystals into tiny pieces, i.e., microseeds.[1] However, special handling is required because protein crystals are soft, fragile, sensitive to changes in their surroundings, and in some cases very small (≤100 μm per dimension). To overcome such difficulties in microseeding of protein crystals, we came up with the use of light.

The use of laser or incoherent light has shown promise as a noncontact means for spatiotemporally controlling crystallization in solutions.[2−14] In particular, we previously demonstrated the microseeding of urea crystals in supersaturated solutions by femtosecond laser ablation.[7] We ablated a small region (1 μm^2) of a urea crystal by the irradiation with a near-infrared femtosecond laser pulse. A single, newly formed urea crystal appeared near the laser focal spot on the original (mother) crystal and grew independently. We found that a single crystal fragment that was the same size as the laser focal spot was ejected, which then acted as the seed crystal.

For the work reported herein, we applied our microseeding technique to protein crystallization, which is generally a more challenging undertaking than is crystallization of a simple organic molecule, e.g, urea. Given the physical characteristics of femtosecond laser listed below, we assumed that the microseeding technique can also be used for protein crystallography. (1) Focused irradiation with a near-infrared (λ = 800 nm)

Received: January 6, 2012
Revised: May 30, 2012
Published: July 11, 2012

   dx.doi.org/10.1021/cg300018t | *Cryst. Growth Des.* 2012, 12, 4334−4339

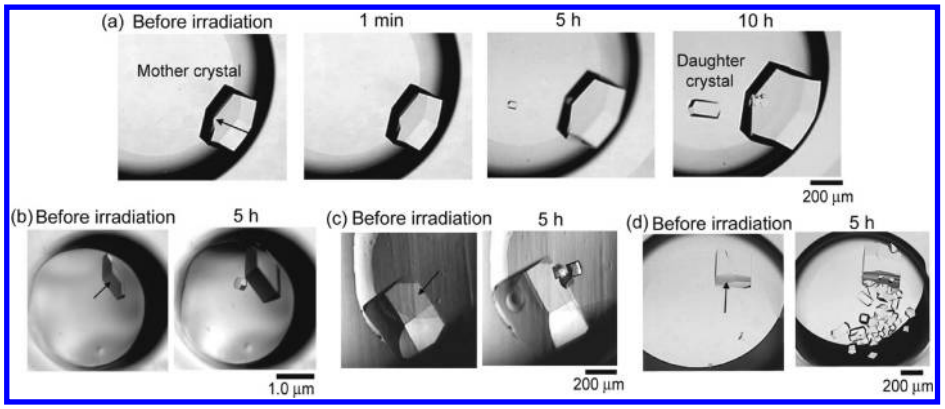

Figure 1. Growth of HEWL microcrystals produced by femtosecond laser ablation. A single femtosecond laser pulse with an energy of (a and b) 0.2 μJ, (c) 0.3 μJ, or (d) 0.4 μJ was directed at the (a and c) {110} or (b and d) {101} face of a tetragonal HEWL crystal that had been grown for 17 h in a supersaturated solution of HEWL (35 mg/mL). The arrows point to the positions on the mother crystals where the laser was focused.

femtosecond laser induces ablation via multiphoton absorption, which should enable the spatially precise isolation of seed crystals from an arbitrary area of the mother crystals while present in a supersaturated solution. Conversely, irradiation with a deep-UV laser cannot reach a protein crystal in a supersaturated solution, owing to the high absorption of UV light by the protein solute.[15] The dimension of spatial accuracy of femtosecond laser ablation via multiphoton absorption is similar to that of the laser focal spot, ~1 μm, which is small enough to precisely target the mother crystals. (2) Femtosecond laser ablation produces less heat than does ablation by other lasers with longer pulse width. The mechanism of femtosecond laser ablation just above the ablation threshold fluence is ascribed to a photomechanical process;[16−19] mechanical stress is confined to the excited region of mother crystals and disrupts the surface, resulting in collective ejection of crystal fragments. There are a significant number of experimental proofs that femtosecond laser ablation occurs at energy densities much smaller than those required for boiling and vaporization.[16−19] Hence, photomechanical ablation reduces potential thermal damage to seed crystals, so to say, "soft" microseeding for protein crystals.

In this work, we have developed a spatially precise, soft microseeding technique that uses femtosecond laser ablation to produce single, high quality protein crystals. To show the general utility of the technique, we used acriflavine resistance protein B (AcrB) as a representative membrane protein in addition to the water-soluble protein, hen egg-white lysozyme (HEWL). AcrB was chosen because crystallization of membrane proteins is in general difficult and extremely dependent on environmental conditions.[20] In addition to the preparation of microseeds, we also tried to control the shape of the tetragonal HEWL seed crystals by adjusting the time interval between initiation of crystallization and laser irradiation. Finally, we assess the impact of photomechanical ablation on the production of high quality seed crystals of proteins by characterizing the ablated crystal surfaces using an atomic force microscope (AFM) and a laser confocal microscopy combined with differential interference microscopy (LCM-DIM) technique.[21,22]

EXPERIMENTAL SECTION

Crystal Preparation. Hen egg-white lysozyme, six-times recrystallized, was purchased from Seikagaku and used without further purification. A solution containing 40−100 mg/mL HEWL and 100 mM sodium acetate, pH 4.5, was mixed (1:1, v/v) with a solution containing 10 wt % NaCl, 100 mM sodium acetate, pH 4.5. The initiation of crystallization, $t = 0$, was defined as the time when the two solutions were mixed. The supersaturated solutions (5 μL each) were individually added into wells of a microbatch plate (Hampton Research) and then covered with 10 μL of paraffin oil (Hampton Research). The plate was incubated at 20 °C. Micrometer-sized crystals appeared within a few hours. HEWL concentrations were determined by optical absorption at 280 nm using an extinction coefficient of 2.64 mL cm^{-1} mg^{-1} using a UV−vis spectrometer (Shimazu, UV-3100).

The preparation of His-tagged AcrB for crystallography has been described in the previous literature.[23] A solution containing 28 mg/mL histidine-tagged AcrB (supersaturated), 20 mM sodium phosphate, pH 6.2, 10% (v/v) glycerol, 0.2% (w/v) dodecylmaltoside was mixed (1:1, v/v) with 16% polyethylene glycol 2000, and 80 mM sodium phosphate, 20 mM sodium citrate-HCl, pH 6.1, to prepare 5 μL samples for crystallization. The AcrB crystals were grown in the wells of a 96-well microbatch plate at 25 °C without covering with paraffin oil. Micrometer-sized crystals appeared within a few hours. The solvent content of the AcrB crystals was calculated using the Matthews program (Collaborative Computational Project No. 4).

Femtosecond Laser Ablation. Plates containing the mother crystals were individually mounted on the stage of an upright microscope (Olympus, BX50). A single pulse from a regeneratively amplified Ti: sapphire laser (800 nm, 120 fs, 1 kHz; Spectra Physics, Hurricane) was passed through an objective lens (Olympus, 10×, numerical aperture = 0.25) and focused on a surface of a crystal. The temperature was maintained at 20 and 25 °C for HEWL and AcrB, respectively. The intensity distributions of the laser pulses were a radial Gaussian. The diameter of the focused spot can be calculated by the diffraction limit (1.22λ/N.A. = 3.8 μm). After irradiation, the crystallization plates were returned to their respective incubators. Microscopic images were acquired using a CCD camera (Ikegami, ICD-878) attached to the microscope.

X-ray Diffraction. Diffraction data were collected on Rigaku R-AXIS IV^{+2} imaging plates at 100 K. Cu Kα radiation was produced using a Rigaku UltraX18 rotating anode generator operated at 50 kV and 100 mA. The detector was positioned 150 mm away from a crystal, and the time per image and the crystal oscillation angle were 30 min and 2°, respectively. The X-ray beam diameter was 0.3 mm. Nonablated regions of the mother crystal were exposed to the X-ray beam.

Crystal Surface Characterization by AFM and LCM-DIM. HEWL (50 mg/mL) was crystallized in 100 mM sodium acetate (pH 4.5), 3 wt % NaCl. The tetragonal HEWL crystals were incubated at 20 °C for several months. The crystals in their crystallization medium were transferred to a cell made of a glass plate (0.15 mm thickness) and silicon rubber walls (0.5 mm thickness). A single femtosecond laser pulse was focused on a HEWL crystal surface. To avoid

dx.doi.org/10.1021/cg300018t | Cryst. Growth Des. 2012, 12, 4334−4339

evaporation of the crystallization media, the cell was covered with paraffin oil or a glass coverslip for AFM or LCM-DIM experiments, respectively. The glass cells were placed onto a self-made unit that used a Peltier element for temperature control. The crystal surfaces etched by the laser irradiation were observed in a saturated solution using an atomic force microscope (Digital Instruments, Nanoscope IIIa) operated at 20 °C. Growth of the {110} face was visualized at 18 °C *in situ* by a LCM-DIM system.[21,22] The LCM-DIM system visualizes crystal surfaces with a resolution much finer than the height of an elementary growth step of tetragonal HEWL crystals (5.6 nm).

RESULTS AND DISCUSSION

Figure 1 shows snapshots of HEWL crystals produced by femtosecond laser ablation. When a 0.2-μJ femtosecond laser pulse was focused on the {110} face of a tetragonal HEWL mother crystal, the crystal surface was etched. Five hours later, a new crystal (daughter crystal) 50 μm in size was observed (Figure 1a). The shape of the daughter crystals was tetragonal, and the crystal grew to ~200 μm within 10 h. Daughter crystals were not obtained when the laser pulse energy was <0.2 μJ, which should be a threshold laser energy for producing daughter crystals. The AFM images also indicated that this pulse energy was the minimum needed for ablation (see below). The energy density at the center point of the focused radial Gaussian beam was ~3.6 J/cm^2, which is the same order of magnitude as that used previously for that of urea microseeding experiments (~2.2 J/cm^2).[7] A 0.2-μJ pulse of laser irradiation at the {101} face of the mother crystal also produced a tetragonal seed crystal (Figure 1b). The number of daughter crystals increased as the laser energy increased (Figure 1c and d). After being irradiated with a 0.2-μJ pulse, the surfaces of mother crystals tended to become smoother with time, whereas polycrystals grew on mother crystal surfaces in the case of higher energies.

The quality of the daughter and mother crystals shown in Figure 1b was evaluated by X-ray diffraction. The diffraction pattern of the daughter crystal did not contain split spots, indicating that it was a single crystal (Figure 2a). The crystallographic parameters for the daughter crystal, e.g., the space group and unit-cell parameters, were almost the same as those for the mother crystals (Figure 2b). Notably, the daughter crystal diffracted to nearly the same resolution (1.47 Å) as the mother crystal did (1.46 Å), even though the daughter crystal was less than half the size of the mother crystal, suggesting that the quality of the daughter crystal was similar to that of the mother crystals.

As a more challenging example, we used polycrystals of AcrB,[23] which, as a membrane protein, is much more difficult to crystallize in a suitable form.[20] The left panel of Figure 3 shows an AcrB polycrystal that had nucleated and grown spontaneously. When the crystal was irradiated with a 0.3-μJ laser pulse which was just above their ablation threshold (~0.2 μJ), isolated daughter crystals were found in solution, as is the case in HEWL. The daughter crystals grew to ~100 μm within 9 h and look like single trigonal crystals of AcrB (right panel in Figure 3). AcrB crystals contained ~90% water, which made the production of seed crystals more difficult than for the HEWL system. Nevertheless, given our ability to produce AcrB daughter crystals, femtosecond laser ablation has the potential to produce microseeds for other recalcitrant proteins.

The shape of the tetragonal HEWL crystals could be controlled by microseeding in solutions that contained different HEWL (supersaturated) concentrations. Figure 4a shows how the shape of daughter HEWL crystals depended on the time

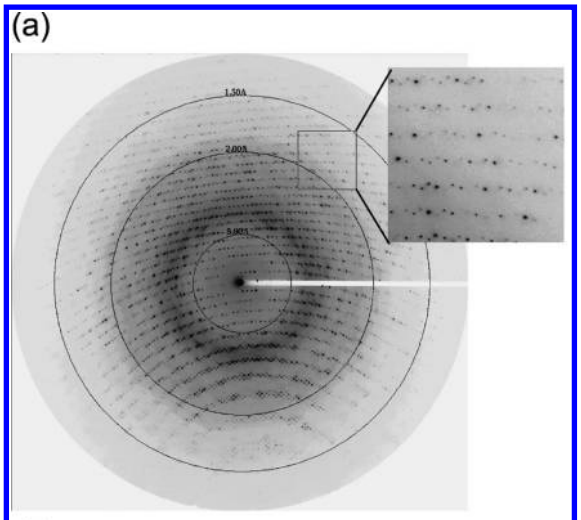

	Mother crystal	Daughter crystal
Space group	$P4_32_12$	$P4_32_12$
Unit-cell parameters (Å)		
a	78.5563±0.0002	78.8892±0.0003
c	36.9859±0.0002	37.1072±0.0001
Resolution (Å)	1.46	1.47
Unique Reflections	20735	19764
R_{merge} (%)	4.9 (23.9)	4.1 (29.5)
Completeness (%)	99.3	99.9

Figure 2. (a) Representative X-ray diffraction pattern of the daughter crystal shown in Figure 1b which was produced by a single 0.2 μJ femtosecond laser pulse. (b) Crystallographic parameters for the diffraction pattern shown in Figure 2a and those for the diffraction pattern of the mother crystal. Values in parentheses are for the highest-resolution shell.

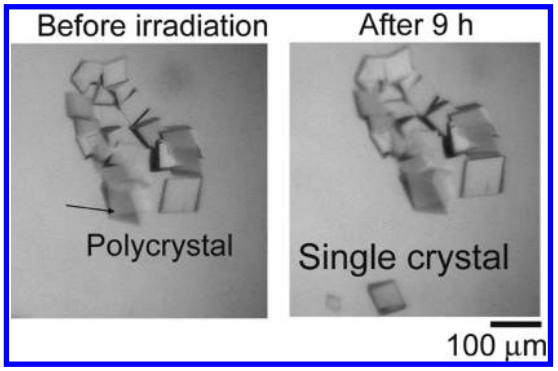

Figure 3. Single crystal of the membrane protein, AcrB, isolated from the mother polycrystal by a single 0.3 μJ femtosecond laser pulse. The arrows point to the positions on the mother crystals where the laser was focused.

interval between initiation of crystallization and laser irradiation. In all cases, the ratio of the *c* axis length (W) to the crystal length along the axis perpendicular to the *c* axis (L) on the {110} face of daughter crystals was smaller than that of the corresponding mother crystals, and it decreased as the time interval increased. The decrease in the W/L radio is attributed to the fact that the growth rate of the{110} face is slower than that of the {101} face at lower supersaturated protein concentrations.[24] In fact, the protein concentration of the

dx.doi.org/10.1021/cg300018t | *Cryst. Growth Des.* 2012, 12, 4334−4339

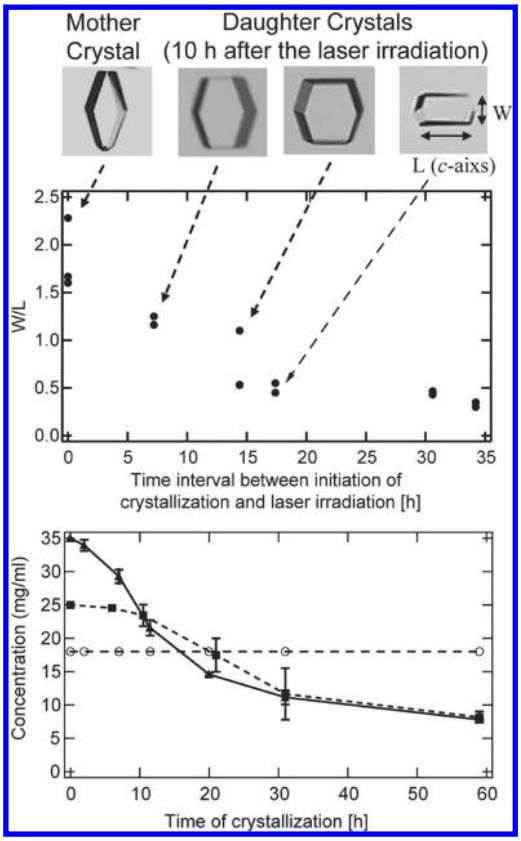

Figure 4. Shape control of tetragonal daughter crystal. (a) The ratio of the crystal length of the {110} *c* axis to the crystal length perpendicular to the *c* axis (W/L) for mother and daughter HEWL crystals as a function of the time interval between initiation of crystallization and laser irradiation. The HEWL mother crystals, grown in a supersaturated solution (35 HEWL mg/mL), were irradiated with a 0.2 μJ laser pulse. W and L were measured 10 h after irradiation. (b) Changes in HEWL concentrations with time. The concentrations were measured as described in the Experimental Section. The initial concentrations of the solutions were 35 mg/mL (triangles), 25 mg/mL (squares), and 18 mg/mL (circles). Five solutions were assayed for each datum point. Each point is reported as the mean ± standard deviation.

solution decreased with time, owing to spontaneous nucleation of additional crystals when the initial protein concentration was >18 mg/mL (Figure 4b). Because the shape of protein crystals is generally dependent on protein concentration, ablation at different times and/or different degrees of supersaturation can be used to control the shapes of crystals from microseeds. Such crystal shape control would be very useful to reduce anisotropic X-ray diffraction, which causes inadequate modeling of anisotropy and structural heterogeneity, because the vast majority of proteins (>90%) are solved as a single, average conformation with Gaussian, isotropic thermal motion.[25]

To assess the impact of femtosecond multiphoton, photomechanical ablation on the single crystal growth of microseeds, the surface of an HEWL mother crystal was observed by AFM. Figure 5a shows a representative image of a mother crystal surface etched by a 0.2 μJ pulse. The etching is ~1 μm in diameter, which is much smaller than the laser spot size estimated by the diffraction limit (3.8 μm). Because HEWL crystals do not absorb 800 nm light, the region of the crystals impinged upon the center of the laser spot is instead excited by mutiphoton absorption, which decreases the diameter of the

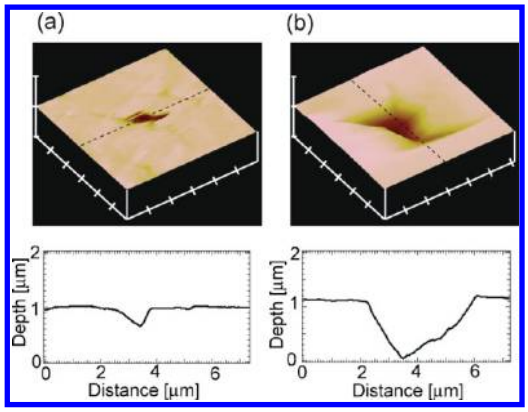

Figure 5. (Top) AFM images of the {110} faces of HEWL crystals in saturated solutions that were irradiated with a femtosecond laser pulse of energy (a) 0.2 μJ and (b) 0.4 μJ in equilibrated (saturated) solutions. (Bottom) Depth profiles along the dotted line in the AFM images.

etching in comparison with etching formed by linear absorption. Figure 5b shows a crystal surface etched by a 0.4 μJ pulse. In that case, the diameter of the etching is ~3 μm, and surface cracking occurred outside the laser-irradiated area. Notably, swelling was not observed surrounding the etched area. Visualization of the subsequent crystal growth on the etched surface at the elementary growth step level by LCM-DIM[21,22] enabled further characterization of laser ablation of HEWL crystals (Figure 6). After a shot of the 0.2 μJ pulse, the

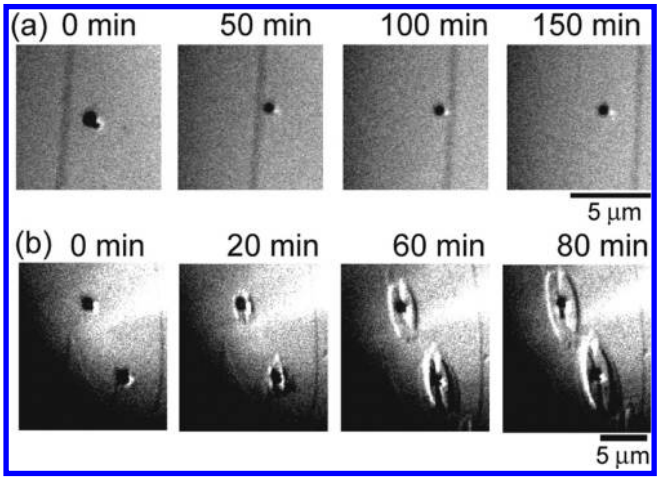

Figure 6. LCM-DIM images of crystal growth on the surface of a HEWL crystal that was etched by a femtosecond laser pulse with energy (a) 0.2 μJ or (b) 0.4 μJ.

etching gradually decreased in size and did not interfere with advancing elementary growth steps (Figure 6a). Conversely, when etched with the 0.4 μJ pulse, bulky islands with heights greater than that of elementary steps were observed at the circumference of the etching, which grew in two dimensions (Figure 6b).

The sharp etching and the cracking of the crystal surface in Figure 5 strongly indicate that the crystal surface is mechanically disrupted via the photomechanical process. The lack of swelling around the etched surface clearly indicated that a thermal effect is not significantly involved and that HEWL molecules are not heat denaturated. The smooth recovery of a

dx.doi.org/10.1021/cg300018t | *Cryst. Growth Des.* 2012, 12, 4334−4339

crystal surface after a shot of the 0.2 μJ pulse (Figure 6B) suggests that the crystalline structure is still retained.

Laser ablation based on photomechanical processes lead to ejection of bulky crystal fragments,[16−19,26] which can act as seed crystals in supersaturated solutions.[7] The number of ejected fragments increases as the laser energy does. Consequently, the number of daughter crystals increases. Crystal fragments that are ejected from a mother crystal should grow into single crystals. Conversely, when deposited on the mother crystal surface, fragments form polycrystals. The bulky islands with heights larger than that of the elementary growth steps (Figure 6b) are probably the result of crystal fragment deposition, because spontaneous two-dimensional (2D) nucleation rarely occurs under the supersaturation condition.

In order to consider the initial size of daughter crystals, we calculate the critical cluster radius required for homogeneous 3D nucleation at t = 35 h, which is the longest time interval between initiation of crystallization and laser irradiation in this study. Considering for simplicity that nuclei are spherical, the Gibbs free energy (ΔG) of a 3D cluster is[27]

$$\Delta G = \frac{4\pi r^3}{3\nu}\Delta\mu + 4\pi r^2\gamma \quad (1)$$

where r is the radius of the cluster, $\Delta\mu$ is the chemical potential difference between molecules in the crystal and the solution, γ is the surface free energy of a 3D cluster (0.62−0.64 mJ/m^2),[22,28] and ν is the molar volume occupied by a growth unit (molecule) in the crystal, which is given by the ratio between the unit cell volume (237.1 Å^3)[27] and the number of molecules per unit cells (8 molecules/unit). By differentiating eq 1, r^*, the critical cluster radius required for 3D nucleation, is expressed as

$$r^* = \frac{2\nu\gamma}{\Delta\mu} = \frac{2\nu\gamma}{kT\log_e\frac{C}{C_e}} \quad (2)$$

Taking C (HEWL concentration) ∼ 10 mg/mL at t = 35 h (Figure 3B) and C_e (equilibrium HEWL concentration) ∼ 2.5 mg,[29] the critical cluster radius required for 3D nucleation under the conditions can be estimated to be ∼7 nm, which corresponds to a cluster of ∼50 molecules. The production of such a bulky protein crystal fragment by femtosecond laser ablation should be a photomechanical process.

CONCLUSIONS

Femtosecond laser ablation of protein crystals is a promising technique as spatially precise, soft microseeding for the production of single protein crystals. The focused irradiation of a femtosecond laser enables us to isolate protein microcrystals with high spatial accuracy in supersaturated solutions through multiphoton processes. Photomechanical ablation processes are very useful for the production of high quality protein seed crystals. Additionally, this microseeding technique will also be useful to control protein crystal shape. We previously found that femtosecond laser-induced cavitation bubbles can trigger nucleation at low supersaturation conditions,[4,14] which should substantially improve the crystal quality of various biological compounds, e.g., drug targeted proteins.[30] Thus, the implementation of controlled nucleation and crystal growth by femtosecond laser ablation will enhance structure-based protein studies, heretofore considered extremely difficult, if not impossible.

AUTHOR INFORMATION

Corresponding Author

*E-mail: hiroshi@mail.saitama-u.ac.jp. Tel/Fax: +81-48-858-3814 (H.Y.Y.); hosokawa@hskw.jp (Y.H.); masuhara@masuhara.jp (H.M.).

Notes

The authors declare no competing financial interest.

ACKNOWLEDGMENTS

The present work was partly supported by grants from Japan Society for the Promotion of Science (KAKENHI No. 24656006, 24680050, 24106505, and 23850006), The Murata Science Foundation, The Mazda Foundation, and Joint Research Program of the Institute of Low Temperature Science (Hokkaido University) to H.Y.Y. Also it was partly supported by the MOE-ATU project (National Chiao Tung University) from the Ministry of Education of Taiwan to H.M.

REFERENCES

(1) McRee, D. E. *Practical Protein Crystallography*, 2nd ed.; Academic Press: San Diego, 1999.
(2) Garetz, B. A.; Aber, J. E.; Goddard, N. L.; Young, R. G.; Myerson, A. S. *Phys. Rev. Lett.* **1996**, *77*, 3475−3476.
(3) Garetz, B. A.; Matic, J.; Myerson, A. S. *Phys. Rev. Lett.* **2002**, *89*, 175501−1−5.
(4) Adachi, H.; Takano, K.; Hosokawa, Y.; Inoue, T.; Mori, Y.; Matsumura, H.; Yoshimura, M.; Tsunaka, Y.; Morikawa, M.; Kanaya, S.; Masuhara, H.; Kai, Y.; Sasaki, T. *Jpn. J. Appl. Phys., Part 2* **2003**, *42*, L798−L800.
(5) Okutsu, T.; Furuta, K.; Terao, M.; Hiratsuka, H.; Yamano, A.; Ferte, N.; Veesler, S. *Cryst. Growth Des.* **2005**, *5*, 1393−1398.
(6) Yoshikawa, H. Y.; Hosokawa, Y.; Masuhara, H. *Jpn. J. Appl. Phys., Part 2* **2006**, *45*, L23−L26.
(7) Yoshikawa, H. Y.; Hosokawa, Y.; Masuhara, H. *Cryst. Growth Des.* **2006**, *6*, 302−305.
(8) Okutsu, T. *J. Photochem. Photobiol.* **2007**, *8*, 143−155.
(9) Sugiyama, T.; Adachi, T.; Masuhara, H. *Chem. Lett.* **2007**, *36*, 1480−1481.
(10) Tsuboi, Y.; Shoji, T.; Kitamura, N. *Jpn. J. Appl. Phys., Part 2* **2007**, *46*, L1234−L1236.
(11) Yoshikawa, H. Y.; Murai, R.; Maki, S.; Kitatani, T.; Sugiyama, S.; Sazaki, G.; Adachi, H.; Inoue, T.; Matsumura, H.; Takano, K.; Murakami, S.; Sasaki, T.; Mori, Y. *Appl. Phys. A: Mater. Sci. Process.* **2008**, *93*, 911−915.
(12) Duffus, C.; Camp, P. J.; Alexander, A. J. *J. Am. Chem. Soc.* **2009**, *131*, 11676−11677.
(13) Yoshikawa, H. Y.; Murai, R.; Sugiyama, S.; Sazaki, G.; Kitatani, T.; Takahashi, Y.; Adachi, H.; Matsumura, H.; Murakami, S.; Inoue, T.; Takano, K.; Mori, Y. *J. Cryst. Growth* **2009**, *311*, 956−959.
(14) Murai, R.; Yoshikawa, H. Y.; Takahashi, Y.; Maruyama, M.; Sugiyama, S.; Sazaki, G.; Adachi, H.; Takano, K.; Matsumura, H.; Murakami, S.; Inoue, T.; Mori, Y. *Appl. Phys. Lett.* **2010**, *96*, 043702.
(15) Kitano, H.; Adachi, H.; Murakami, A.; Matsumura, H.; Takano, K.; Inoue, T.; Mori, Y.; Owa, S.; Sasaki, T. *Jpn. J. Appl. Phys., Part 2* **2004**, *43*, L73−L75.
(16) Zhigilei, L. V.; Garrison, B. J. *J. Appl. Phys.* **2000**, *88*, 1281−1298.
(17) Hosokawa, Y.; Yashiro, M.; Asahi, T.; Masuhara, H. *J. Photochem. Photobiol., A* **2001**, *142*, 197−207.
(18) Paltauf, G.; Dyer, P. E. *Chem. Rev.* **2003**, *103*, 487−518.
(19) Vogel, A.; Venugopalan, V. *Chem. Rev.* **2003**, *103*, 577−644.
(20) DeLucas, L. *Membrane Protein Crystallization*; Academic Press: 2009.
(21) Sazaki, G.; Tsukamoto, K.; Yai, S.; Okada, M.; Nakajima, K. *Cryst. Growth Des.* **2005**, *5*, 1729−1735.

(22) Van Driessche, A. E. S.; Sazaki, G.; Otalora, F.; Gonzalez-Rico, F. M.; Dold, P.; Tsukamoto, K.; Nakajima, K. *Cryst. Growth Des.* **2007**, *7*, 1980−1987.
(23) Murakami, S.; Nakashima, R.; Yamashita, E.; Yamaguchi, A. *Nature* **2002**, *419*, 587−593.
(24) Durbin, S. D.; Feher, G. *J. Cryst. Growth* **1986**, *76*, 583.
(25) DePristo, M. A.; de Bakker, P. I. W.; Blundell, T. L. *Structure* **2004**, *12*, 831−838.
(26) Asahi, T.; Yoshikawa, H. Y.; Yashiro, M.; Masuhara, H. *Appl. Surf. Sci.* **2002**, *197*, 777−781.
(27) Garcia-Ruiz, J. M. *J. Struct. Biol.* **2003**, *142*, 22−31.
(28) Galkin, O.; Vekilov, P. G. *J. Am. Chem. Soc.* **2000**, *122*, 156−163.
(29) Van Driessche, A. E. S.; Gavira, J. A.; Lopez, L. D. P.; Otalora, F. *J. Cryst. Growth* **2009**, *311*, 3479−3484.
(30) Adachi, H.; Murakami, S.; Niino, A.; Matsumura, H.; Takano, K.; Inoue, T.; Mori, Y.; Yamaguchi, A.; Sasaki, T. *Jpn. J. Appl. Phys., Part 2* **2004**, *43*, L1376−L1378.